

Electronic Structure of the Si(100) Surface A Defects Analyzed by Scanning Tunneling Spectroscopy at 80 K

Yasuyuki SAINOO¹, Tomohiko KIMURA¹, Ryuji MORITA¹, Mikio YAMASHITA²,
Kenji HATA¹ and Hidemi SHIGEKAWA^{1,2,*}

¹Institute of Applied Physics and CREST, Japan Science Technology Cooperation, University of Tsukuba, Tsukuba 305-8573, Japan

²Department of Applied Physics, CREST, Japan Science Technology Cooperation, Hokkaido University, Sapporo, 060-8628, Japan

³Department of Chemistry and Biotechnology, Graduate School Engineering, University of Tokyo, Tokyo 113-8656, Japan

(Received February 23, 1999; accepted for publication March 30, 1999)

The A defects on the Si(100) surface can be classified as A_1 , A_2 , and A_3 at low temperatures. We carried out scanning tunneling microscopy observations and scanning tunneling spectroscopy measurements at ~ 80 K to study their electronic structures. We found that the A_1 defect is semiconductive similar to the A defect at room temperature (RT), while the A_2 and A_3 defects exhibited states in the surface band gap at 80 K. On comparing these results with the theoretical models, we concluded that the A_1 defect correspond to the Rebonded vacancy model. The broken vacancy model and the twisted vacancy models are the possible candidates for the A_2 and A_3 defects, respectively.

KEYWORDS: scanning tunneling microscopy, scanning tunneling spectroscopes, surface electronic phenomena, silicon, surface defects

1. Introduction

One of the prominent features of the Si(100) surface is the atomic level defects. From scanning tunneling microscopy (STM) studies, typical defects on this surface were classified by Hamers and Kohler¹ as types A, B, and C. Among them, the A defect seems to have the simplest structure; a single vacancy defect, as observed by STM in both filled and empty state images. Some structural models have been proposed from the theoretical studies, and the dimer vacancy (DV) model is most widely accepted.^{2–5} However, the A defect structure still remains to be determined.

The DV model denotes a structure with a single dimer vacancy which is formed by the simple removal of a dimer from a perfectly reconstructed Si(100) surface. Wang *et al.* proposed two structures for the DV model.³ When a single dimer is removed, the second layer atoms can either move apart, or move together to form bonds across the introduced gap, was first suggested by Pandey.⁴ Moreover, Owen *et al.* proposed that the DV model is divided into three subcategories:⁵ (1) Rebonded model (R-DV model, Fig. 1(a)): second layer atoms form two bonds across the gap. (2) Twisted model (T-DV model, Fig. 1(b)): a single bond is formed across the gap, and two dangling bonds remain. (3) Broken model (B-DV model, Fig. 1(c)): second layer atoms do not form any bonds, and they relax away from the center of the defect.

According to the ab initio total-energy study of the DV defect by Wang *et al.*, the R-DV model has no states in the lower half of the surface band gap. Hamers and Kohler experimentally performed current-voltage (I-V) measurements at RT, and obtained the result that the A defect has a clear surface band gap, although it is somewhat reduced in magnitude compared to the surface band gap. Owen *et al.* also demonstrated that the low-bias STM image is in good agreement with the simulated STM image, based on the R-DV model. Based on this consistency observed between theoretical and experimental results, the R-DV model is widely accepted to explain the structure of the A defect.

On the other hand, it is well known that defects influence

the characteristic configuration of the surrounding dimers. At RT, symmetric dimers are observed mostly on the Si(100) surface. From the total-energy calculations, a bucked dimer is found to be more stable than symmetric dimers. In fact, a phase transition occurs around 200 K, and buckled dimers begin to be observed. Yokoyama and Takayanagi⁶ reported that symmetric dimers are induced, even at ~ 140 K, on both sides of the A defect. This result also seems to support the structure of the R-DV model.

However, from the detailed analysis of the effect of the A defect on the surrounding dimer configurations at 80 K, Uchikawa *et al.* found that the A defect can be classified as A_1 , A_2 , and A_3 at ~ 80 K.⁷ However, their structures and relation to the A defect have not yet been clarified. In order to determine the structures, information about their electronic structures is essential.

In this study, we conducted STM observations and scanning tunneling spectroscopy (STS) measurements at ~ 80 K. We found that (1) the A_1 defect has a clear surface band gap, although it is somewhat reduced in magnitude compared to the surface band gap, and (2) the A_2 and A_3 defects have states in the surface band gap. Therefore, we concluded that the A_1 defect corresponds to the rebonded vacancy model, and the A_2 and A_3 defects correspond to the broken vacancy model and the twisted vacancy model, respectively.

2. Experimental

Si samples were phosphorous-doped with a conductivity of $0.005 \Omega \text{ cm}$. After the samples were prebaked at $\sim 700^\circ\text{C}$ for ~ 12 h, they were flashed once to 1250°C for 30 sec, followed by a slow cool down. The base pressure was kept under 5×10^{-8} Pa during flashing. An electrochemically etched tungsten tip was used for the STM observations.

3. Result and Discussion

3.1 Characteristics of the A_1 , A_2 , and A_3 defects

First, we show the A_1 , A_2 , and A_3 defects which were observed at ~ 80 K. STM images and schematics of the stick and ball structures of the A_1 , A_2 , and A_3 defects are shown in Figs. 2(a), 2(b), and 2(c), respectively. The A_1 defect, as shown in Fig. 2(a), suppresses buckling on both its sides, and

*E-mail address: hidemi@ims.tsukuba.ac.jp, <http://dora.ims.tsukuba.ac.jp>

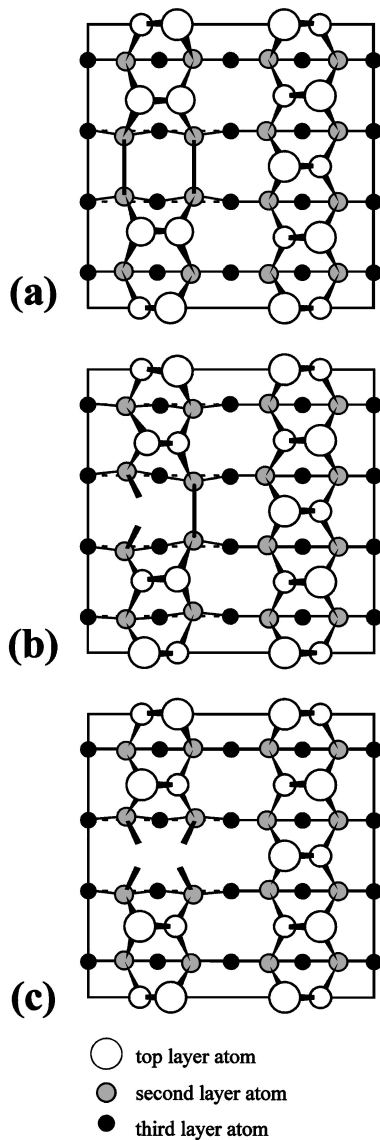


Fig. 1. Defect structures of (a) Rebonded dimer vacancy model (R-DV model), (b) Twisted dimer vacancy model (T-DV model), (c) Broken dimer vacancy model (B-DV model).

induces a symmetric dimer structure. The A_2 defect does not disturb the antiferromagnetic ordering of the buckled dimers on both its sides (see Fig. 2(b)). The A_3 defect does not suppress the buckling on both its sides, but it disturbs the antiferromagnetic ordering of the buckled dimers (see Fig. 2(c)). Namely, the A_3 defect is a phase shifter. At 80 K, A_1 defects were frequently observed. However, the A_2 defect occurred less frequently than the A_1 defect. Moreover, the A_3 defect was rarely observed. The A_3 defect looks to appear to occur on a higher defect density surface.

3.2 Spectroscopic analysis of the A_1 , A_2 , and A_3 defects

We measured the tunneling I-V characteristics of the A_1 , A_2 , and A_3 defects, as shown in Figs. 3(a), 3(c), and 3(e). All I-V measurements were carried out at the center of the vacancy. The solid lines in Fig. 3 denote the I-V curves measured for the defects. In each case, the tunneling I-V characteristic of the normal dimers was measured with the same tip apex and is denoted in Fig. 3 as a dashed line. Tunneling spectra of the dimers were taken to confirm that the STS

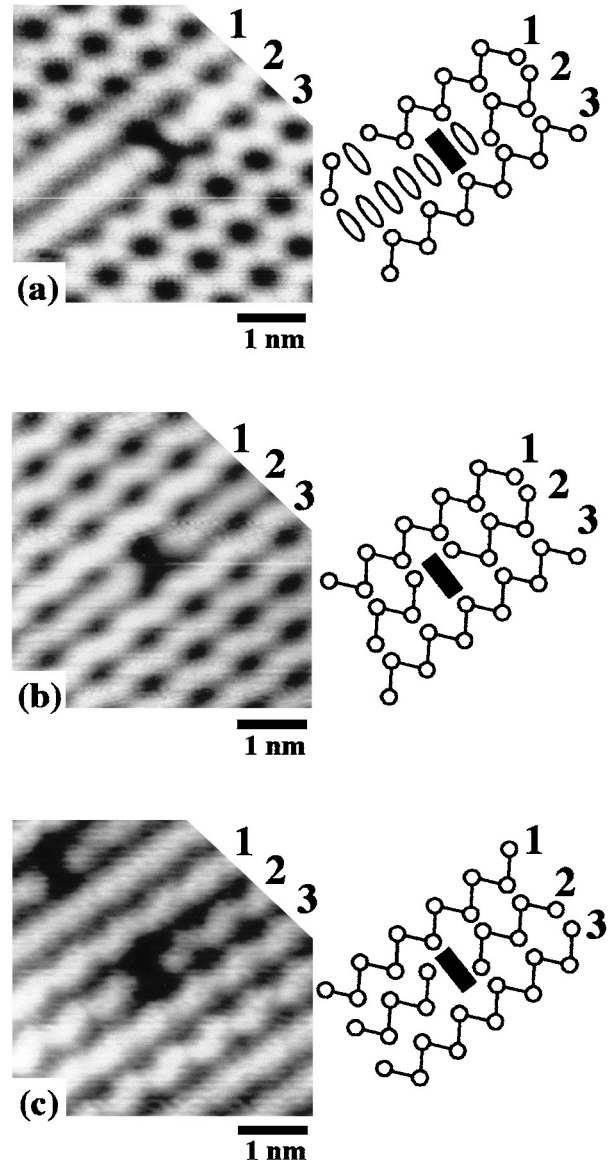


Fig. 2. STM images and the stick and ball structures of the A_1 , A_2 , and A_3 defects in (a), (b) and (c), respectively. All STM images were taken at sample bias -1.0 V and tunneling current 1.0 nA.

measurements are not influenced by the electronic structure of the tips. Here, they show a semiconductive feature with a band gap of -0.5 V, which is in accordance with previous results.^{1,8)} Here, we address the issue of the reliability of STS measurements. It is well known that STS measurements are subject to the conditions of the tunneling tip. One type of tip apex will provide reproducible STS spectra, although a different tip apex might produce very different results. Regarding this point, before and after the transitions, STS measurements were conducted on the normal dimers, and we confirmed that each STS spectrum had a similar shape to the spectrum reported by Hamers *et al.*⁸⁾ The spectrum of the dimers obtained by Hamers (and by us) is consistent with many experimental results and is believed to represent the true electronic characteristics. We discussed the characteristic of each spectrum in comparison with that of the normal dimer. By this procedure, we can safely confirm that all of the STS measurements were conducted with the similar tip conditions and that the experimental results were not devalued by the possible

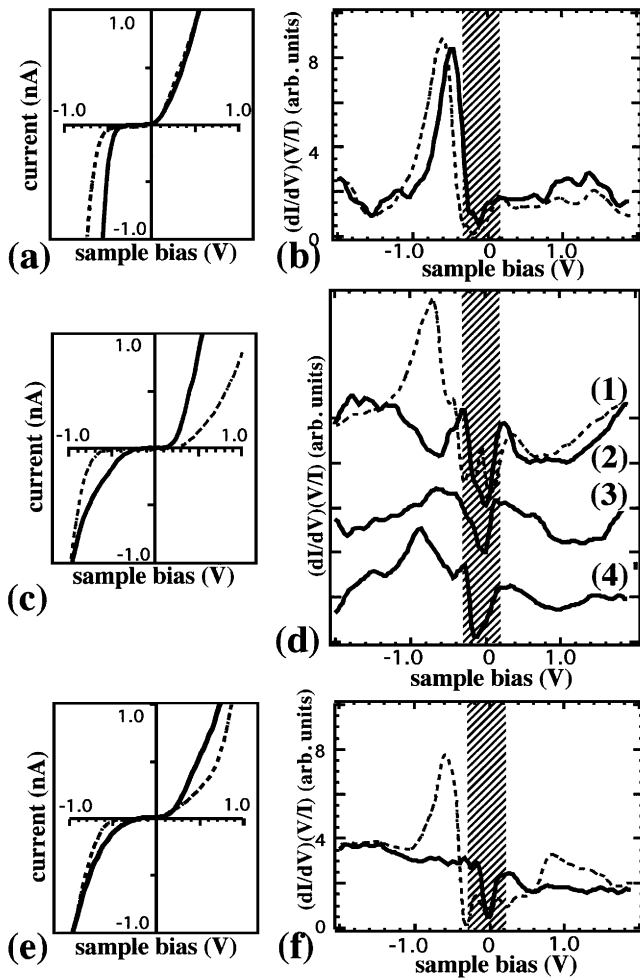


Fig. 3. I-V and STS spectra obtained for the A_1 (a), (b), A_2 (c), (d) and A_3 (e), (f), respectively. The dashed lines denote the spectra obtained for the normal dimers taken with the same tip apex. The spectra (2)–(4) in (d) represents the typical spectra obtained for the A_2 defects in different areas. The shaded regions in (b), (d) and (f) represent the energy window in which reliable STS signals could not be obtained because of the emphasized tunneling noise.

electronic structure of the tips.

As shown in Fig. 3(a), the A_1 defect always had a surface band gap, whose width was around ~ 0.4 V, slightly smaller than that of the normal dimers. Thus, the A_1 defect has a semiconductive characteristic even at 80 K. Regarding the A_2 defect, the surface band-gap width seemed to be slightly scattered, however, it was much narrower than that of the A_1 defect. In a specific case, the defect showed a metallic feature (see Fig. 3(c)). The A_3 defect did not exhibit a surface band gap, and it was always metallic (see Fig. 3(e)).

In order to discuss the electronic structures in more detail, the normalized tunneling conductivities (STS spectra, $(dI/dV)/(I/V)$ versus V) in the range from -2 V to $+2$ V were numerically calculated from the tunneling I-V curves in Fig. 3. The corresponding STS spectra of the A_1 , A_2 , and A_3 defects are displayed in Figs. 3(b), 3(d), and 3(f), respectively. The normalization procedure of the tunneling current significantly emphasizes the tunneling noise (\sim several pA) around the Fermi level, preventing observation of the intrinsic electronic structure near the Fermi level. The shaded regions in Fig. 3 represent the energy window in which no reliable STS signals could be obtained because of the emphasized tunnel-

ing noise.

As denoted by the solid line in Fig. 3(b), the A_1 defect has three dominant energy states at ~ 0.5 V, ~ 0.2 V and ~ -1.0 V. In comparison with the STS spectrum obtained for a normal dimer, STS characteristics are almost the same in both cases. This result is in good agreement with those obtained by Hamers *et al.* as the I-V characteristic of the A defect at RT.

The STS spectra of the A_2 defects were slightly scattered as mentioned above, which is denoted by the solid lines in Figs. 3(d)-(2)-(4). However, in comparison with the STS spectra of the normal dimers, STS spectra of the A_2 defect generally showed a weaker peak at the filled state, and a larger peak at the empty state side near the Fermi level.

As denoted by the solid line in Fig. 3(f), the STS spectra of the A_3 defect did not show any characteristic peaks like the A_1 and A_2 defects, and were completely metallic. The spectral intensity was weak compared to those of the others.

Filled- and empty-state STM images of the A_1 defect at ~ 80 K are shown in Figs. 4(a) and 4(b), respectively. As shown in Fig. 4(a), symmetric dimers are observed on both sides of the defect in the filled-state image. However, at the positions of the symmetric dimers in the filled-state image, four separated atoms were observed in the empty-state STM image as shown in Fig. 4(b).

Current imaging tunneling spectroscopy (CITS) was performed on an A_1 defect, and Fig. 4(d) schematically shows the spectra taken at the positions shown in Fig. 4(c). Numbering of the spectra correspond to the positions of which the data were taken. The spectra were averaged over an area of approximately 0.16×0.16 nm².

STS spectra in Fig. 4(d) show a surface band gap of ~ 0.4 V. This is narrower compared to the value of the normal dimer, ~ 0.5 V, but the characteristic is clearly semiconductive. As shown in Fig. 4(d), the dominant peak in the filled-state area shifted toward the position observed for the normal dimer as the measured position which is away from the defect.

Since symmetric dimers theoretically have a metallic feature, the observed semiconductive STS spectra do not agree with this feature.

3.3 Structural models for the A_1 , A_2 , and A_3 defects from the analysis at 80 K

In this section, we discuss the appropriate structural models for the A_1 , A_2 , and A_3 defects observed at ~ 80 K.

The A_1 defect is a “single dimer vacancy”, and apparent symmetric dimers are observed on both sides of the vacancy. Moreover, the results of the I-V measurements of the A_1 defect at ~ 80 K shows a clear surface band gap. These results are in good agreement with the results of the I-V measurements of the A defect at RT by Hamers and Kohler¹⁾ and the calculated density of states performed for the “rebonded vacancy model” by Wang *et al.*³⁾ Thus, we conclude that the A_1 defect corresponds to the “rebonded vacancy model”.

On the other hand, buckled dimers are observed on both sides of the A_2 and A_3 defects, and the A_2 and A_3 defects show some density of states near the Fermi level. Thus, the A_2 and A_3 defects are considered to have different structures from those based on the R-DV model. However, since symmetric dimers are observed on both sides of the A defect at RT, it is possible that A_2 and A_3 defects have the same origin

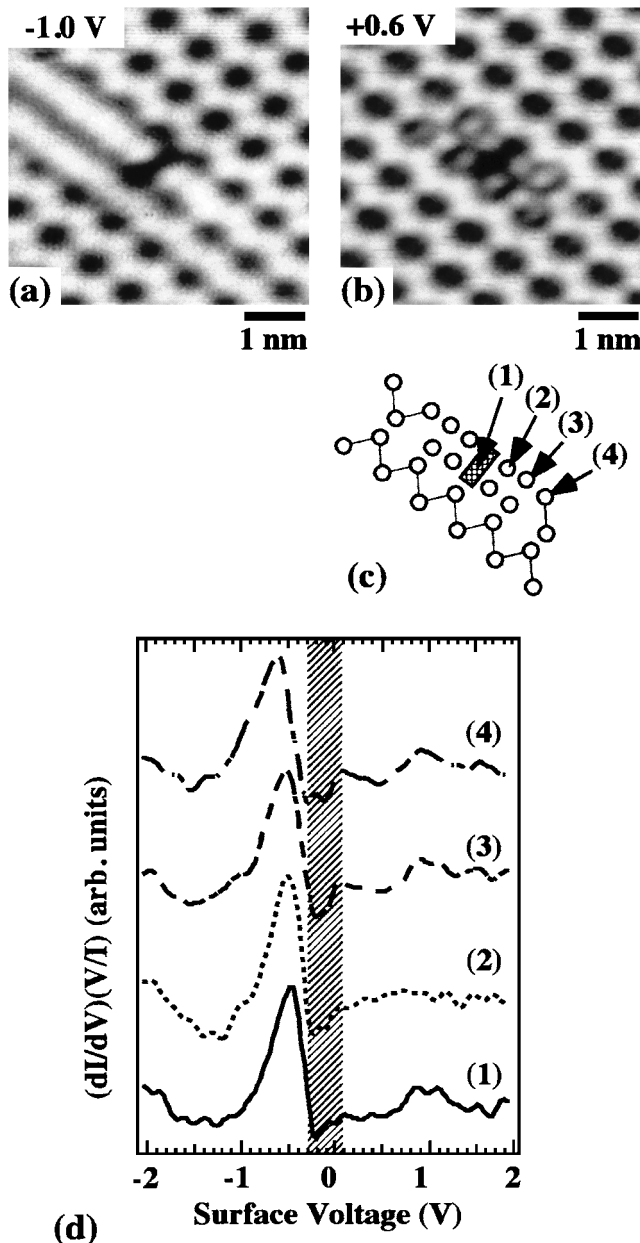


Fig. 4. Filled (a) (sample bias -1.0 V and tunneling current 1.0 nA) and empty (b) ($+0.6$ V, 1.0 nA) STM images of the A_1 defect. (c) a stick and ball structure around a A_1 defect. (d) STS spectra taken at the positions shown in (c).

as the A_1 defect. At a low temperature such as 80 K, dimers are buckled and have a high-ordering among them; $c(4 \times 2)$ or $p(2 \times 2)$ arrangements. Thus the configuration of dimers on both sides of the defects must be strongly affected by the surrounding dimer arrangement. Namely, the bonding structure in the underlying layer is expected to be affected by the strain induced by the surrounding dimer arrangement. In the scheme of the dimer vacancy model, the structure of the B-RV model has some density of states near the Fermi level, as calculated by Wang *et al.*³⁾ Therefore, taking account of the rather free bonding condition in the underlying layer, the B-RV model is a possible candidate for the structures of the A_2 defect. In consideration of the structure of the underlying layer, the T-RV model may be attributed to the A_3 defect. In order to discriminate between the A_2 and A_3 defects in more detail, further study, including theoretical analysis, is essential.

4. Conclusion

We conducted STM observation and STS measurements at ~ 80 K to study the electronic structure of the A_1 , A_2 , and A_3 defects. We found that the A_1 defect has a semiconductive characteristic similar to that observed at RT. However, the A_2 and A_3 defects showed the existence of some states in the surface band. In comparison with the theoretical results by Wang *et al.*,³⁾ we concluded that the A_1 defect corresponds to the rebonded vacancy model. The broken vacancy model and the twisted vacancy model are possible candidates for the A_2 and A_3 defects, respectively.

Acknowledgments

This work was supported by a Grant-in-Aid for Scientific Research from the Ministry of Education, Science, Sports and Culture of Japan.

- 1) R. J. Hamers and U. K. Kohler: *J. Vac. Sci. Technol. A* **7** (1989) 2854.
- 2) S. Ihara, S. L. Ho, T. Uda and M. Hirao: *Phys. Rev. Lett.* **65** (1990) 1909.
- 3) J. Wang, T. A. Arias and D. J. Jonannpoulos: *Phys. Rev. B* **47** (1993) 10497.
- 4) K. C. Pandey: *Proc. 17th Int. Conf. on the Physics of Semiconductors*, eds. D. J. Chadi and W. A. Harrison; (Springer, New York, 1985) p 55.
- 5) J. H. G. Owen, D. R. Bowler, C. M. Goringe, K. Miki, G. A. D. Broggs: *Surf. Sci.* **341** (1995) L1042.
- 6) T. Yokoyama and K. Takayanagi: *Phys. Rev. B* **56** (1997) 10483.
- 7) M. Uchikawa, M. Ishida, K. Miyake, K. Hata, R. Yoshizaki and H. Shigekawa: *Surf. Sci.* **357-358** (1996) 468.
- 8) R. J. Hamers, Ph. Avouris and F. Bozso: *Phys. Rev. Lett.* **59** (1987) 2071.